Molecular Crystals and Liquid Crystals

Publication details, including instructions for authors and subscription information:
http://www.tandfonline.com/loi/gmcl20

Design of Siloxane Liquid Crystals Forming a De Vries SmA* Phase

G. Galli [a], M. Reihmann [a], A. Crudeli [a], E. Chiellini [a], Yu. Panarin [b c], J. Vij [b], C. Blanc [d], V. Lorman [d] & N. Olsson [e]

[a] Dipartimento di Chimica e Chimica Industriale and INSTM - UdR Pisa, Università di Pisa, Pisa, Italy

[b] Department of Electronic and Electrical Engineering, Trinity College, Dublin, Ireland

[c] School of Electronics and Communication Engineering, Dublin Institute of Technology, Dublin, Ireland

[d] GDPC, UMR and LPMT, UMR, Université Montpellier II, France

[e] Department of Materials and Surface Chemistry, Chalmers University of Technology, Göteborg, Sweden

Version of record first published: 31 Aug 2006

To cite this article: G. Galli, M. Reihmann, A. Crudeli, E. Chiellini, Yu. Panarin, J. Vij, C. Blanc, V. Lorman & N. Olsson (2005): Design of Siloxane Liquid Crystals Forming a De Vries SmA* Phase, Molecular Crystals and Liquid Crystals, 439:1, 245/[2111]-257/[2123]

To link to this article: http://dx.doi.org/10.1080/15421400590958089

Mol. Cryst. Liq. Cryst., Vol. 439, pp. 245/[2111]–257/[2123], 2005

ISSN: 1542-1406 print/1563-5287 online
DOI: 10.1080/15421400590958089

Design of Siloxane Liquid Crystals Forming a De Vries SmA* Phase

G. Galli
M. Reihmann
A. Crudeli
E. Chiellini
Dipartimento di Chimica e Chimica Industriale and INSTM – UdR Pisa, Università di Pisa, Pisa, Italy

Yu. Panarin
Department of Electronic and Electrical Engineering, Trinity College, Dublin, Ireland and School of Electronics and Communication Engineering, Dublin Institute of Technology, Dublin, Ireland

J. Vij
Department of Electronic and Electrical Engineering, Trinity College, Dublin, Ireland

C. Blanc
V. Lorman
GDPC, UMR and LPMT, UMR, Université Montpellier II, France

N. Olsson
Department of Materials and Surface Chemistry, Chalmers University of Technology, Göteborg, Sweden

We designed and synthesized new SmA liquid crystals with different molecular architectures based on the chiral mesogen MR11, which was unsubstituted, or attached at one end and at both ends of a trisiloxane segment in the monosubstituted MSi3-MR11 and disubstituted DSi3-MR11 siloxanes, respectively. We studied the critical divergence of the magnetic susceptibility by measurements of the induced tilt angle θ_{ind} at the SmA*–SmC* transition. While all three SmA* liquid crystals presented a de Vries character, this was quite distinctive for DSi3-MR11 for which the critical exponent $\gamma = 1.87$ was maximal. X-ray diffraction experiments*

This work was supported by the EU Contract *SAMPA* (HPRN-CT-2002–00202).
Address correspondence to G. Galli, Dipartimento di Chimica e Chimica Industriale and INSTM–UdR Pisa, Università di Pisa, 56126 Pisa, Italy. E-mail: gallig@dcci.unipi.it

confirmed that the SmA–SmC* transition occurred with essentially no layer shrinkage.*

Keywords: de Vries smectic; electrooptics; molecular design; siloxane liquid crystal

INTRODUCTION

The liquid crystalline SmA phase is described as a 2D layered structure where the molecular director is perpendicular to the smectic layer plane. On cooling down to the SmC phase, the molecular director becomes tilted with respect to the smectic layer normal which leads to a layer shrinkage. In real SmA liquid crystals the molecules are not exactly perpendicular to the smectic layer planes due to (at least) non-perfect molecular shape. Nevertheless, most SmA liquid crystals are consistent with such "rigid-rod" microscopic molecular model and undergo a smectic layer shrinkage at the SmA–SmC transition.

On the other hand, in a de Vries SmA phase the molecules are assumed to be tilted similar to the SmC phase in two possible structures [1] in which the tilted layers are stacked in a random fashion, or alternatively the molecules are tilted, but without long-range order in the tilt direction. While the molecular tilt direction is randomly distributed in the SmA state, it becomes ordered below the SmA–SmC transition. In both suggested structures the transition to the SmC phase therefore occurs through an ordering of tilt directions, which would produce no significant shrinkage of the smectic layer spacing.

Recently, there have been several reports dealing with the synthesis and some physical properties, such as birefringence and electroclinic effect, of de Vries SmA* liquid crystals [2–9]. Among them, there are different materials like compounds including organosiloxanes, fluoroethers and chiral lactic esters in the tail. However, up to now there has been no really clarifying explanation reported on why such materials should exhibit de Vries properties. Moreover, there is no general guideline available on how to design a de Vries material starting from typical molecular components of conventional chiral liquid crystals.

In this work we synthesized new SmA* organosiloxanes with varied chemical structure (Scheme 1) and investigated their de Vries character by electrooptical measurements and X-ray diffraction analysis. By comparison with previous results on similar de Vries organosiloxanes [6], we propose a molecular architecture of a disubstituted trisiloxane which seems to be of general advantage to develop de Vries SmA* phases.

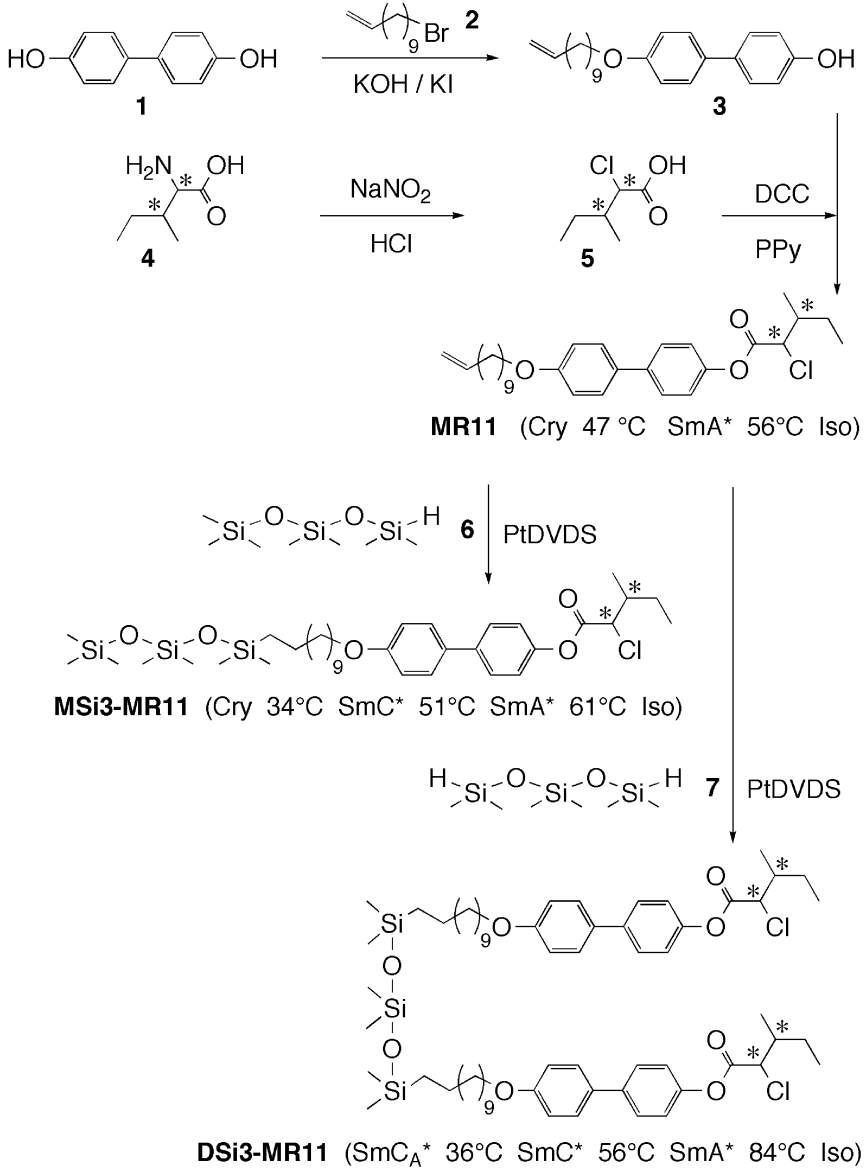

SCHEME 1 Synthesis and transition temperatures of the mesogen MR11 and the trisiloxanes MSi3-MR11 and DSi3-MR11.

EXPERIMENTAL

Materials

All solvents were distilled prior to use. All commercially available chemicals (Sigma-Aldrich, ABCR, Fluorochem) were used as received.

4′-(10-Undecenyl-1-oxy)-4-biphenol (3)

20.00 g (0.11 mol) of 4,4′-biphenol **(1)** was dissolved with 3.5 g (0.62 mol) of KOH and 0.1 g KI in 300 ml methanol. The mixture was heated to 60°C and ethanol was added until a clear solution was obtained. 12.52 g (54 mmol) of 11-bromoundecene (**2**) was then added dropwise and the solution was refluxed for 2 days under a nitrogen atmosphere. The heterogeneous reaction mixture was then poured into water and the precipitate was filtered and dried under vacuum. After recrystallisation from methanol, 12.87 g (70% yield) of pure product was obtained. White crystals, mp 128°C; $R_f = 0.50$ (ethyl acetate/petroleum ether 1:1); FT-IR (KBr) $\tilde{\nu}/cm^{-1}$: 3400–3100 (OH), 3075 (vinyl CH), 2962–2840 (aliphatic CH_2), 1643 (vinyl C=C), 1610, 1503, 1462 (aromatic C=C), 1251 (C–OH), 810 (aromatic); ^{1}H NMR (200 MHz, $CDCl_3$) δ/ppm: 7.46 (d, 2H, H3′, H5′-biphenyl, $J = 8.78$ Hz), Hz), 7.44 (d, 2H, H3, H5-biphenyl, $J = 8.68$ Hz), 6.95 (d, 2H, H2, H6-biphenyl, $J = 8.68$ Hz), 6.89 (d, 2H, H2′, H6′-biphenyl, $J = 8.78$ Hz), 5.93 (m, 1H, CH_2=C<u>H</u>), 5.81 (2d, 2H, C<u>H$_2$</u>=CH), 3.99 (t, 2h, CH_2O), 2.07 (m, 2H, CH_2=C<u>H</u>C<u>H$_2$</u>), 1.81 (m, 2H, C<u>H$_2$</u>CH_2O), 1.32 (12H, aliphatic CH_2).

(S,S)-2-chloro-3-methylpentanoic acid (5)

10.00 g (76.24 mmol) of (*L*)-isoleucine (**4**) was dissolved in 100 ml of 6 N HCL at 0°C and a solution of 6.48 g (76.24 mmol) of $NaNO_2$ in 30 ml water was added dropwise. The solution was then stirred for 4 h at 0°C and then for 15 min at room temperature. The solution was extracted with ethyl acetate and the organic phase was dried with $MgSO_4$ and evaporated under vacuum. The remaining oil was distilled to give 10.2 g (87% yield) of pure product. Colourless oil (90°C/0.02 mbar), $R_f = 0.88$ (ethyl acetate/petroleum ether 1:1); FT-IR (NaCl) $\tilde{\nu}/cm^{-1}$: 3500–2880 (OH, CH_2, CH_3), 1723 (C=O), 1450–1395 (CH_3) 1290–1203 (C–OH), 695 (CCl); ^{1}H NMR (200 MHz, $CDCl_3$) δ/ppm: 11.60–10.20 (1H, COOH), 4.24 (d, 1H, ClC<u>H</u>, $J = 6.70$ Hz), 2.12 (m, 1H, C<u>H</u>CH_3), 1.63 (m, 1H, CH_3C<u>H$_2$</u>), 1.36 (m, 1H, CH_3C<u>H$_2$</u>), 1.07 (d, 3H, C<u>H$_3$</u>CH, $J = 6.70$ Hz), 0.94 (t, 3H, C<u>H$_3$</u>CH_2).

4′-(10-Undecenyl-1-oxy)-4-biphenyl(S,S)-2-chloro-3-methylpentanoate (MR11)

12.00 g (35.4 mmol) of **3**, 5.34 g (35.4 mmol) of **5** and 0.5 g (3.1 mmol) of 4-pyrrolidinopyridine (PPy) were dissolved in 200 mL of dry dichloromethane under a nitrogen atmosphere and cooled to 0°C. 7.31 g (35.4 mmol) of dicyclohexylcarbodiimide (DCC) in 15 mL of dry dichloromethane was added in 30 min and the mixture was then stirred for 2 days at room temperature. The precipitate was filtered and the solution evaporated under vacuum. The solid residue was purified by flash chromatography (silica gel 240–400 mesh) using ethyl acetate/petroleum ether 1:1 as eluent. The resulting solid was further purified by dissolving it in hot petroleum ether, cooling, filtration and evaporation of the petroleum ether under vacuum to give 12.8 g (77% yield) of pure product. White wax, $R_f = 0.82$ (ethyl acetate/petroleum ether 1:4); FT-IR (KBr) $\tilde{\nu}$/ cm^{-1}: 3075 (vinyl CH), 2962–2840 (aliphatic CH), 1745 (C=O), 1650 (vinyl C=C), 1606, 1504, 1465 (aromatic C=C), 1190–1140 (C–O), 950 (vinyl C=C), 820, 800 (aromatic), 695 (CCl). ^{1}H NMR (200 MHz, $CDCl_3$) δ/ppm: 7.57 (d, 2H, H3, H5-biphenyl, $J = 8.96$ Hz), 7.50 (d, 2H, H3′, H5′-biphenyl, $J = 8.78$ Hz), 7.18 (d, 2H, H2, H6-biphenyl, $J = 8.96$ Hz), 6.98 (d, 2H, H2′, H6′-biphenyl, $J =$ 8.78 Hz), 5.83 (m, 1H, CH_2=C$\underline{H}$), 4.99 (2d, 2H, C$\underline{H_2}$=CH), 4.42 (d, 1H, ClCH, $J = 6.70$ Hz), 4.01 (t, 2H, C$\underline{H_2}$O), 2.26 (m, 1H, C$\underline{H}$CH$_3$), 2.07 (m, 2H, CH_2=CHC$\underline{H_2}$), 1.81 (m, 4H, C$\underline{H_2}$CH$_2$O, CH$_3$C$\underline{H_2}$), 1.50–1.34 (12H, aliphatic C$\underline{H_2}$), 1.17 (d, 3H, C$\underline{H}$C$\underline{H_3}$, $J = 6.70$ Hz), 1.01 (t, 3H, C$\underline{H_3}$CH$_2$).

General Procedure for the Preparation of the Siloxanes by Hydrosilylation

250 mg of MR11 was dissolved in 5 mL of dry toluene in a pyrex tube. The solution was degassed and sealed with a septum under a nitrogen atmosphere. An 1.15 molar amount of 1,1,3,3,5,5,5-heptamethyl-1-hydrotrisiloxane (**6**) was added for the synthesis of the monosubstituted trisiloxane, or a 1.8 molar amount of 1,1,3,3,5,5-hexamethyl-1,5-dihydrotrisiloxane (**7**) for the synthesis of the disubstituted trisiloxane. After addition of 6 μL of a 2 wt% xylene solution of platinum-1,3-divinyl-1,1,3,3-tetramethyldisiloxane complex (PtDVDS), The tube was placed in a sonicator for 2–5 h at 30°C. The conversion was followed by FT-IR detecting the progressive decrease of the absorption bands at 2160 cm^{-1} (Si–H) and 950 cm^{-1} (vinyl C=C). Upon completion of the reaction, the solvent was evaporated and the residue was dissolved in dichloromethane and precipitated in cold methanol. The final product was further purified as specified below.

1,1,3,3,5,5,5-Heptamethyltrisiloxane 1-[4′-(undecyl-1-oxy)-4-biphenyl(S,S)-2-chloro-3-methylpentanoate] (MSi3-MR11)

Flash chromatography ($R_f = 0.86$ ethyl acetate/petroleum ether 1:8), 38% yield; FT-IR (KBr) $\tilde{\nu}/cm^{-1}$: 3100–3000 (aromatic CH), 2980–2880 (aliphatic CH), 1766 (C=O), 1607, 1524, 1469 (aromatic C=C), 1290 (O–CO), 1256 (C–OH), 1168 (C–O), 800 (aromatic); ^{1}H NMR (200 MHz, $CDCl_3$) δ/ppm: 7.58 (d, 2H, H3, H5-biphenyl, $J = 8.96$ Hz), 7.51 (d, 2H, H3′, H5′-biphenyl, $J = 8.78$ Hz), 7.18 (d, 2H, H2, H6-biphenyl, $J = 8.96$ Hz), 6.98 (d, 2H, H2′, H6′-biphenyl, $J = 8.78$ Hz), 4.42 (d, 1H, CLCH, $J = 6.70$ Hz), 4.02 (t, 2H, CH_2O), 2.26 (m, 1H, $C\overline{H}CH_3$), 1.83 (m, 4H, $C\overline{H}_2CH_2O$, $CH_3C\overline{H}_2$), 1.42–1.24 (16H, aliphatic $\overline{C}H_2$), 1.17 (d, 3H, $\overline{C}HC\underline{H}_3$, $J = 6.70$ Hz), 1.02 (t, 3H, $C\underline{H}_3CH_2$), 0.55 (m, 2H, $SiCH_2$), 0.11, 0.08, 0.05 (21H, $SiCH_3$).

1,1,3,3,5,5-Hexamethyltrisiloxane 1,5-bis-[4′-(undecyl-1-oxy)-4-biphenyl(S,S)-2-chloro-3-methylpentanoate] (DSi3-MR11)

Repeated precipitations from chloroform solutions into methanol; 67% yield; FT-IR (KBr) $\tilde{\nu}/cm^{-1}$: 3100–3000 (aromatic CH), 2980–2880 (aliphatic CH), 1760 (C=O), 1607, 1527, 1475 (aromatic C=C), 1285 (O–CO), 1252 (C–OH), 1172 (C–O), 829 (aromatic); ^{1}H NMR (200 MHz, $CDCl_3$) δ/ppm: 7.58 (d, 4H, H3, H5-biphenyl, $J = 8.96$ Hz), Hz), 7.51 (d, 4H, H3′, H5′-biphenyl, $J = 8.78$ Hz), 7.18 (d, 4H, H2, H6-biphenyl, $J = 8.96$ Hz), 6.99 (d, 4H, H2′, H6′-biphenyl, $J = 8.78$ Hz), 4.42 (d, 2H, ClCH, J = 6.70 Hz), 4.02 (t, 4H, CH_2O), 2.27 (m, 2H, $C\overline{H}CH_3$), 1.81 (m, 8H, $C\underline{H}_2C\underline{H}_2O$, $CH_3C\underline{H}_2$), 1.48–1.22 (32H, aliphatic $C\overline{H}_2$), 1.18 (d, 6H, $CHC\underline{H}_3$, $J = 6.70$ Hz), 1.02 (t, 6H, $C\underline{H}_3CH_2$), 0.56 (m, 4H, $SiCH_2$), 0.09–0.05 (18H, $SiCH_3$).

Characterization

The electrooptical measurements were performed in a conventional cell (thickness either 15 μm or 9 μm), In which both ITO layers were coated with Nissan 1266 polymer to ensure planar alignment. The cell was filled with the liquid crystal in its isotropic state and then cooled down very slowly to the SmA^* phase. An AC field ($U = 10$ V, $f = 20$ Hz) was applied perpendicular to the cell confining plates. The signal from a photodetector was measured by a lock-in amplifier ensuring high signal to noise ratio. The measured voltage was converted to the induced tilt angle θ_{ind} by comparing with a switching angle measured at the same applied voltage and temperature. Then, the temperature dependence of θ_{ind} was fitted to a power law to evaluate the critical exponent γ, as discussed below.

X-Ray diffraction spectra were recorded on cooling the liquid crystal samples from the isotropic phase in Lindman capillaries. The Cu-Kα radiation ($\lambda = 1.54$ Å) (rotating anode) was used. The detector was a 2D plate (Imageplate) which allowed 2D powder spectra to be obtained. After angular integration, the X-ray diffraction spectra presented well pronounced smectic peaks. The peak position was precisely located by fitting locally the peak with a Lorentzian and a base line. The relative position of the peak for each sample was quite precise, and the error bars in the presented graphs correspond to this relative error.

RESULTS AND DISCUSSION

We synthesized three chiral liquid crystals MR11, MSi3-MR11, and DSi3-MR11 viable to form an SmA* phase at reasonably low temperatures (Scheme 1). The basic mesogenic core of MR11 consisted of a biphenyl 2-chloro-3-methylpropionate unit, that is also known to favor the SmC–SmA phase sequence [10]. Two different chemical structures of organosiloxanes were derived from MR11 by a platinum(0)-catalyzed hydrosilylation reaction [10,11]: a chiral mesogen was linked to one end of a trisiloxane segment in MSi3-MR11 (monosubstituted) or at both ends in DSi3-MR11 (disubstituted). Thus, the effect of the flexible siloxane component on the SmA* behavior of the varied molecular architectures could be assessed.

The three molecules all displayed an SmA* phase, but linking the mesogen to either trisiloxane segment in MSi3-MR11 and DSi3-MR11 changed the thermal characteristics of the materials notably. In both siloxanes there existed an SmC* phase (Fig. 1), which was not present in MR11, and the SmA*–isotropic phase transition rose to higher temperatures. This was due to a stabilization of the smectic phase probably by an intramolecular phase segregation of the incompatible siloxane segment. Conversely, the onset temperature of the SmA* phase was not affected significantly (Scheme 1). The siloxane liquid crystals appeared, therefore, more suitable for characterization and application.

The potential de Vries character of liquid crystals may be studied conveniently by investigating the temperature dependence of the susceptibility in the SmA* phase. This method is based on the concept that, at the SmA*-SmC* transition temperature T_C [12,13], the correlation between the tilt directions diverges by different laws $\xi \sim (T–T_C)^{-\nu}$ for orthogonal and de Vries SmA* phases, although the order parameter symmetry is the same in both cases. Under idealized conditions of two extreme options of SmA* liquid crystals, the transition

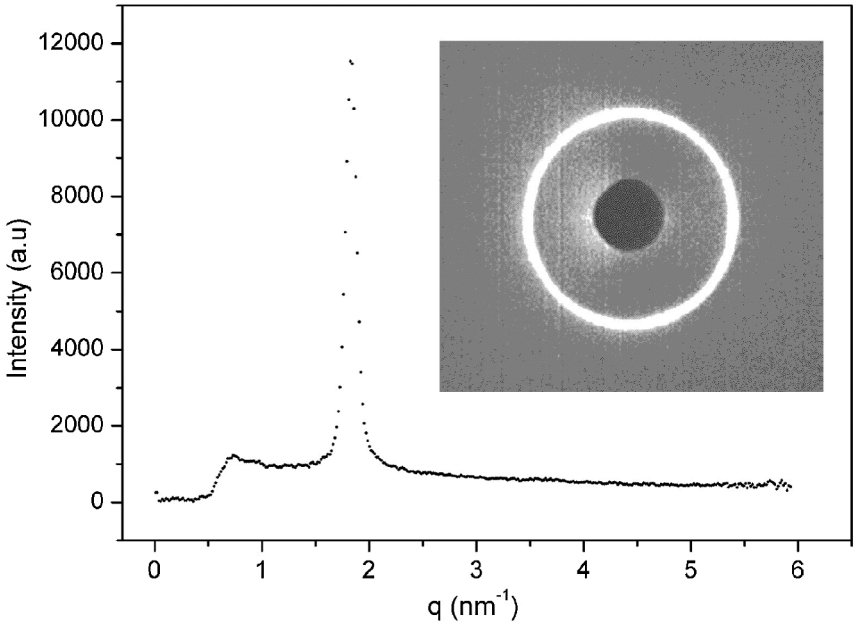

FIGURE 1 Angular integration of the 2D powder X-ray diffraction spectrum (inset) of the SmC* phase of DSi3-MR11 at 50°C ($d = 34.3$ Å).

mechanism in an orthogonal SmA* is due to an induced molecular tilt on the one hand, whereas in the de Vries phase it is due to the rotation of molecules around a cone on the other hand. Consequently, the respective phase transitions belong to two different universality classes and should show quite different critical indices. In particular, the susceptibility diverges by a power law $\chi \sim (T - T_C)^{-\gamma}$, in which the critical exponent is 1.33 for an orthogonal SmA* or 2 for a de Vries SmA*. However, in real SmA* phases the transition can take place as a combination of both mechanisms. The value of γ can then manifest a more or less pronounced degree of de Vries character for a given mesogen [4].

Following this approach, we measured the electrooptical response, θ_{ind}, and monitored its temperature dependence in the SmA* phase to evaluate γ. The electrooptical response for MR11 is shown in Figure 2. This was fitted with a power law with a critical exponent $\gamma = 1.53$, although the extrapolated critical temperature T_C of 34°C occurred in the crystalline phase. Thus, the SmA*–SmC* transition was a virtual one in MR11.

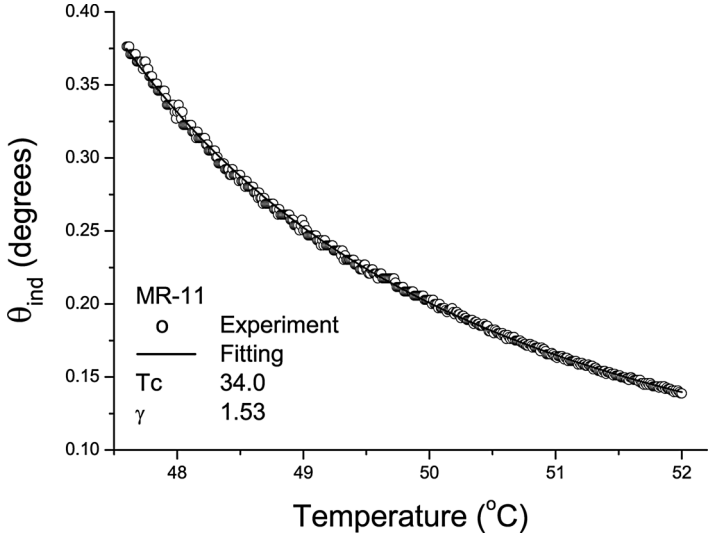

FIGURE 2 Electrooptical response in the SmA* phase of the mesogen MR11 ($E = 1\,V/\mu m$).

Interestingly, the electrooptical response of MSi3-MR11 and DSi3-MR11 revealed different γ-values (Fig. 3), and accordingly different de Vries properties, despite the fact that both materials are very similar from a chemical viewpoint. For the trisiloxane MSi3-MR11, carrying one mesogen, γ was 1.53. The values of γ for both MR11 and MSi3-MR11 are comparable to those found for other de Vries SmA* molecules that contain one or no siloxane segment [4,6].

By contrast, the trisiloxane DSi3-MR11, having two mesogens attached, displayed a much greater γ of 1.87 (Fig. 3). This value indicates that DSi3-MR11 should possess a quite distinct de Vries SmA* phase. Such a conclusion was also supported by our X-ray diffraction results. Figure 4 illustrates the change of the smectic layer periodicity d with temperature for DSi3-MR11. The SmA*-SmC* transition was sluggish with a small shortening of d, which varied by only 3% over the entire smectic range from 80°C down to 30°C.

We very recently found [6] analogous electrooptical and X-ray diffraction behaviors at the SmA*–SmC* transition in trisiloxane DSi3-AC11 (Fig. 5). The determined value of γ was as high as 1.96, indicating a practically pure de Vries scenario [6]. In complete contrast, the unsubstituted mesogen AC11 and the monosubstituted disiloxane MSi2-AC11 presented γ of 1.66 and 1.49, respectively [6].

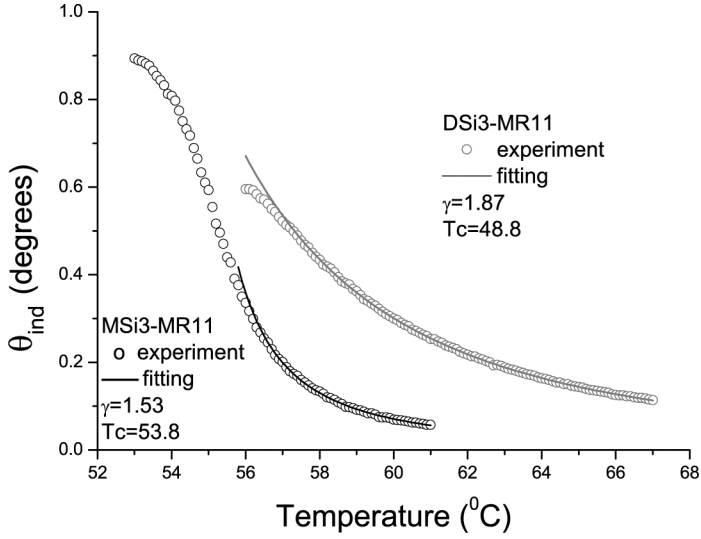

FIGURE 3 Electrooptical response in the SmA* phase of the trisiloxanes MSi3-MR11 and DSi3-MR11 (E = 1 V/μm).

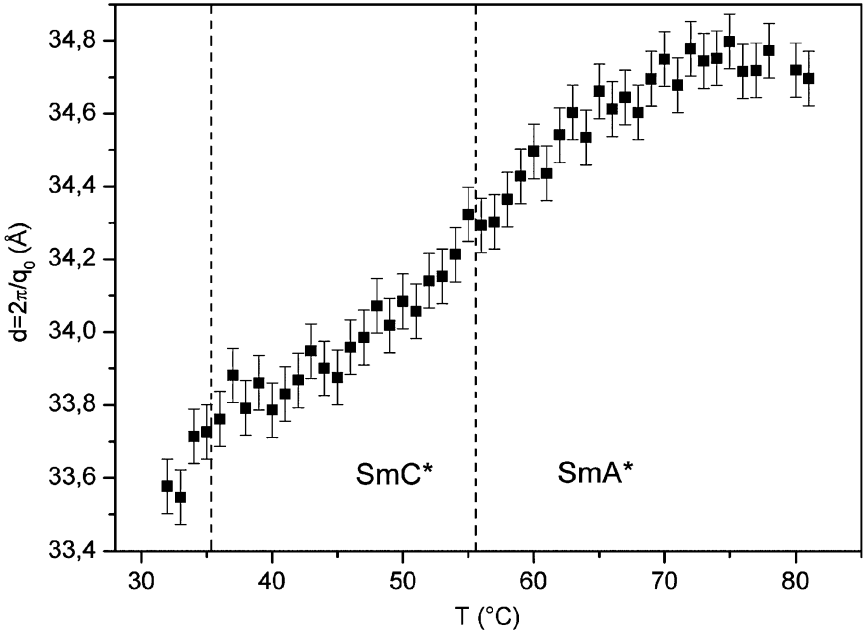

FIGURE 4 Variation of the smectic layer periodicity with temperature for DSi3-MR11.

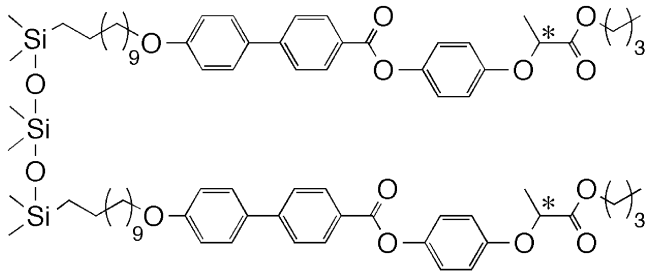

DSi3-AC11 (Cry 30 °C SmX 80 °C SmC* 122 °C SmA* 131 °C Iso)

FIGURE 5 Structure and phase transitions of the trisiloxane DSi3-AC11 [6].

From these results we conclude that the molecular architecture of the siloxanes DSi3-MR11 and DSi3-AC11, both consisting of two lateral mesogenic cores interconnected by a central trisiloxane spacer segment, is of significant advantage in realizing an SmA phase of the de Vries type. While this propensity was inherent in the mesogens MR11 and AC11, it was optimized in the disubstituted siloxanes. In fact, simple incorporation of a peripheral siloxane segment in MSi3-MR11 or MSi2-AC11 did not result in an enhancement of γ.

These findings may be of general relevance and require further discussion. The measured smectic layer periodicity d of around 34 Å for DSi3-MR11 corresponds roughly to half length of the (isolated) molecule ($L/2 \approx 30$ Å) evaluated by an AM1 energy-minimized model (Fig. 6). Similar results were previously found for DSi3-AC11 ($d = 35$ Å, $L/2 \approx 35$ Å). This suggests that the trisiloxane molecules are almost completely interdigitated in a monolayer structure in both the SmA* and SmC* phases, which arrangement possibly better accommodates the siloxane segments between the smectic layers. A similar structural model supporting this intramolecular segregation was recently proposed for different disubstituted siloxane liquid crystals [14].

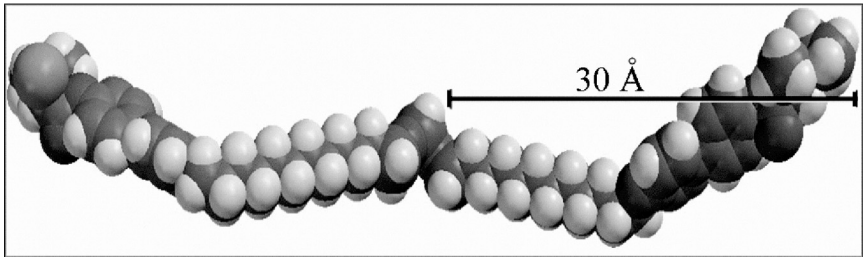

FIGURE 6 Energy-minimized AM1 model of the trisiloxane DSi3-MR11.

As suggested by the energy-minimized AM1 model of DSi3-MR11 (and DSi3-AC11, not shown here), the trisiloxane spacer facilitates an angled disposition of the two mesogens with respect to each other. This might induce a tilted position of the molecules varying from layer to layer and depress the tendency of the material to form an orthogonal SmA phase. The siloxane segment is sufficiently flexible to allow the molecules to adopt easily different positions on their cone. Since the siloxane separates the molecules from each other in a way of microphase segregation, the smectic layers are decoupled from each other. In addition, the tilt direction is randomly distributed within each layer. The decoupling of the layers seems to be a key point in realizing a SmA phase of the de Vries type, since by this means it is possible to eliminate effectively the long-range interlayer correlations.

One should expect that such a structure also favors the formation of an antiferroelectric SmC* phase [14,15]. This is consistent with our observations of this phase for DSi3-MR11 below 36°C. However, we cannot exclude that the siloxane spacer segment can allow the complete folding of the side mesogenic side arms so that they pack nearly parallel to each other in a monolayer smectic structure.

CONCLUSIONS

The new liquid crystals form a de Vries SmA* phase, as suggested by electrooptical and X-ray diffraction measurements. The de Vries character is maximized when two mesogens are interconnected by a sufficiently long and flexible siloxane segment, such as in DSi3-MR11 ($\gamma = 1.87$) and DSi3-AC11 ($\gamma = 1.96$). In this scenario, the siloxane segment favors angled intralayer positions of the mesogens and decouples the smectic layers from each other. The overall result should be that long-range interlayer correlations are effectively eliminated, so that the tilt angle directions adopt a random distribution in passing from layer to layer.

REFERENCES

[1] (a) de Vries, A. (1977). *Mol. Cryst. Liq. Cryst.*, *41*, 27.
(b) de Vries, A. (1979). *J. Chem. Phys.*, *71*, 25.
[2] Panarin, Yu. P., Panov, V., Kalinovskaya, O. E., & Vij, J. K. (1999). *J. Mater. Chem.*, *9*, 2967.
[3] Selinger, J. V., Collings, P. J., & Shashidhar, R. (2002). *Phys. Rev. E*, *64*, 061705.
[4] (a) Naciri, J., Carboni, C., & George, A. K. (2003). *Liq. Cryst.*, *30*, 219.
(b) Carboni, C., Mehdi, R., Gorge, A. K., Al-Harti, S. H., & Naciri, J. (2004). *Mol. Cyst. Liq. Cryst.*, *410*, 61.
[5] Rössle, M., Zentel, R., Lagerwll, J. P. F., & Giesselmann, F. (2004). *Liq. Cryst.*, *31*, 883.

[6] Reihmann, M., Crudeli, A., Blanc, C., Lorman, V., Panarin, Yu., Vij, J., Olsson, N., & Galli, G. (2004). *Ferroelectrics*, *309*, 111.
[7] Radcliffe, M. D., Brostrom, M. L., Epstein, K. A., Rappaport, A. G., Thomas, B. N., Shao, R., & Clark, N. A. (1999). *Liq. Cryst*., *26*, 789.
[8] Giesselmann, F., Zugenmaier, P., Dierking, I., Lagerwall, S. T., Stebler, B., Kaspar, M., Hamplova, V., & Glogarova, M. (1999). *Phys. Rev. E*, *60*, 598.
[9] Naciri, J., Ruth, J., Crawford, G., Shashidhar, R., & Ratna, B. R. (1995). *Chem. Mater*., *7*, 1397.
[10] Chiellini, E., Galli, G., Dossi, E., Cioni, F., & Gallot, B. (1993). *Macromolecules*, *26*, 849.
[11] Svensson, M., Helgee, B., Skarp, K., & Andersson, G. (1998). *Macromol. Chem. Phys*., *199*, 535.
[12] Panarina, O. E., Panarin, Yu. P., Vij, J. K., Spector, M. S., & Shashidhar, R. (2003). *Phys. Rev. E*, *67*, 051709.
[13] de Gennes, P. G. & Prost, J. (1993). *The Physics of Liquid Crystals*, 2nd ed., Oxford University Press: Oxford, UK, 528.
[14] Guillon, D., Osipov, M. A., Mery, S., Siffert, M., Nicoud, J.-F., Bourgogne, C., & Sebastiao, P. (2001). *J. Mater. Chem*., *11*, 2700.
[15] Lehmann, P., Robinson, W. K., & Coles, H. J. (1999). *Mol. Cryst. Liq. Cryst*., *328*, 221.